Pile design for X-rotor offshore wind turbine

Pile design for X-rotor offshore wind turbine

Jing Dong*, Adriana Correia Da Silva, Michael Muskulus

Department of Civil and Environmental Engineering, Norwegian University of Science and Technology NTNU, Trondheim, Norway

E-mail: jing.dong@ntnu.no

Abstract. For the foundations of traditional offshore structures in oil and gas industry, the dominant load is in vertical direction. For wind turbines, especially for vertical axis wind turbines, the lateral loads are increased significantly, which makes them the key element of the pile design. The X-rotor offshore wind turbine is a novel concept which is a hybrid of vertical and horizontal axis wind turbines. This paper aims at giving a detailed solution for the pile design of X-rotor type offshore wind turbines based on the existing guidelines and to gain an insight in the influences of the cyclic loads on the pile parameter selection. The pile capacity design and the pile performance design are executed and then the influence of the piles to the natural frequencies of the wind turbine is evaluated.

1. Introduction

The X-rotor offshore wind turbine (see Figure 1) is a novel wind turbine concept which aims to reduce the cost of energy from offshore wind [1]. It is a hybrid of vertical and horizontal axis wind turbines - the primary rotor is a two-blade (or three-blade) vertical axis rotor and the secondary rotors are horizontal axis rotors which are fixed on the tip of the lower blades of the primary rotor. The turbine is supported by a four-legged jacket substructure.

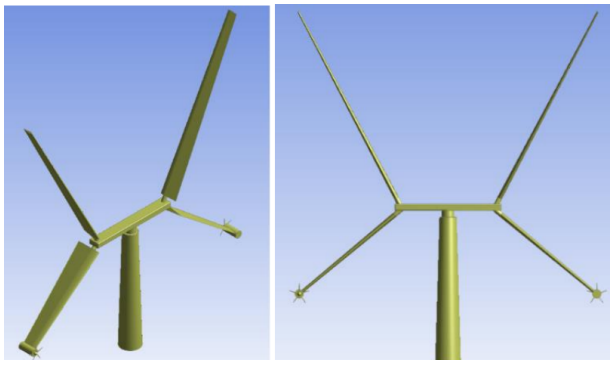

Figure 1: Design representation of the X-Rotor Concept [1]

The structural components of the jacket foundation include the jacket, the piles and the transition piece. Specific load analyses are necessary to be considered for each stage of the life cycle of the jacket including construction, transportation, installation and maintenance. The concept is like this: the space frame of the jacket is prefabricated on shore, and then it is

transported to the site and erected on the seafloor. And then, the piles are driven through sleeves in the jacket, and connected to the sleeves. The transition piece is then mounted on top of the jacket [2].

Offshore piles are typically steel tubular pipes from 1 m to 3 m in diameter and from 40 m to 300 m or more in length. A three or four-legged jacket structure is founded on the seafloor with a single pile placed below each leg. Piles can be distinguished as driven piles, drilled and grouted piles, balled piles and vibro-driven piles. For the convenience of discussion, in this paper only driven piles are considered. Open-ended piles are often used as driven piles. Piles are driven into the seafloor with heavy-energy impact hammers that are capable of executing underwater driving and are less restricted by water depth. So far, hydraulic hammers are the ideal equipment for offshore piling application. In order to use pile materials efficiently it would be recommended to use the smallest diameter that is suitable for the shear and moment loads, and the deepest possible pile penetration. Installation requirements, however, will usually result in a shallower pile of larger diameter [3]. Usually, thicker-wall piles are used to be able to match with heavier hammers to achieve more effective penetration and driving rates [2].

In industry rules, piles are designed to be able to support the platform by bearing the axial loads and lateral loads which are transferred to the piles from the bottom of the platform. The axial loads are considered to be balanced by shaft friction and end bearing resistance of the piles. The lateral loads are considered to be balanced by the piles' bending moments and the support from the soil surrounding the piles.

However, the application of piles to the X-rotor platform [1] makes some new challenges for pile design, which can be described like this: First, the ratio of the lateral load to axial load on the X-rotor platform foundation (more than 1:4 for extreme situations of the current design) is much higher than what applies to the traditional oil and gas platforms that have higher self-weight and lower mass center , which may make the tensile pile capacities more critical. This phenomenon can be explained like this: The axial load is mostly from the self-weight of the structure and equipment. The self-weight of the X-rotor platform is relatively small comparing with that of the O&G platforms from statistic data [2, 4]. On the other hand, the lateral loads are mostly from the wind for the above-water part and from wave for the under-water part of the system. The wind area is large comparing with the structure itself for the X-rotor platform, witch generates relatively high and unsteady aerodynamic loads. Secondly, it is also recognized that the cyclic loads should be considered adequately in the design process [5]. Particularly for the X-rotor platform foundation design, the ratio of the cyclic load to static load is higher than in the situation that applies to oil and gas foundations.

This paper aims to give a detailed solution for the ultimate limit state (ULS) design as part of the pile design of X-rotor type offshore wind turbine, which is mostly based on the existing guidelines, and to gain an insight in the influences of the cyclic loads on the pile parameter selection.

2. Environmental condition and design load case

The X-rotor wind turbine is proposed to be designed for the North Sea Center (NSC) site located at 55.13N, 3.43E as described in [6] with a water depth of 40 m.

2.1. Soil properties

The soils can be classified into sand and normally consolidated to over-consolidated clay at different buried depth. For this project, due to the lack of soil data, a simplified single layer sand soil is considered for the pile design, with the parameters shown in Table 1.

Table 1: Soil data

Type	Friction angle	Saturated unit weight	Effective unit weight
Dense sand	35 degrees	20 kN/m3	10 kN/m3
	Tip bearing factor	Shaft friction limit	Tip resistance limit
	50	115 kPa	12 MPa

2.2. Load case design

To verify the pile capacity and performance for ULS analysis, load cases with power production condition and the parked condition are considered in this paper according to DNVGL-ST-0437 [7], as shown in Table 2.

Table 2: Design load cases

Design situation	DLC	Wind	Wave	Wind and wave directionality
Power production	1	NTM	NSS	0°
	2	NTM[1]	NSS[2]	45°
	3	NTM	NSS	−45°
	4	NTM	NSS	90°
	5	NTM	NSS	−90°
Parked	6	EWM[3]	ESS[4]	0°
	7	EWM	ESS	45°
	8	EWM	ESS	−45°
	9	EWM	ESS	90°
	10	EWM	ESS	−90°

[1] NTM: normal turbulence model.
[2] NSS: normal sea state, joint prob. distribution.
[3] EWM: extreme wind speed model (50-year).
[4] ESS: extreme sea state (50-year).

For the power production condition we use a wind speed of 19 m/s, which is the highest wind speed for the power production condition, in combination with the joint distribution of conditional significant wave height of 4.3 m and an expected conditional peak period of 8.0 s (taken from the design basis [8]). For the parked condition we use the extreme wind speed model wind speed of 36.8 m/s, ESS significant wave height of 10.1 m and peak period of 14.1 s [6].

3. Rules and regulations for pile design

3.1. Ultimate axial pile capacity

Similar rules and regulations for the pile design can be found from DNVGL-ST-0126 [9] and API [10, 11, 12]. Taking API 2GEO for example, firstly the pile capacity is evaluated, which includes the shaft friction capacity and the end bearing capacity. The pile capacity is evaluated based on an ideal assumption of a (quasi-)static and monotonic application of the axial loads and has no reflection on the dynamic interaction between pile and soil during field conditions, as shown in Eq (1).

$$Q_c = Q_{f,c} + Q_p = f(z)A_s + qA_p \tag{1}$$

Where Q_c is the ultimate axial capacity of piles in compression; $Q_{f,c}$ is the shaft friction capacity in compression, in force units; Q_p is the end bearing capacity, in force units; $f(z)$ is the unit shaft friction, in stress units; A_s is the side surface area of the pile; q is the unit end bearing at the pile tip, in stress units; A_p is the gross end area of the pile; z is the depth below the original seafloor.

The most critical ultimate loads should be used to calculated the pile capacity. A critical load case for a four-legged jacket often occurs when the load acts on the frame of the platform in the diagonal direction. In this case, one pile will bear the maximum tension load (or minimum compression load) while the pile on the diagonal will bear most of the compression load [13]. However, for major jackets, mud mats are used on the bottom of the platform to supply adequate area for load distribution to the soil [14]. Mud mats are supposed to be able to temporally support the on-bottom load of the jacket including the dead load and environmental loads before the jacket is pinned onto the seafloor by the piles. Thus, the vertical compression loads can be shared by other bottom structural members of the platform while the pullout tension loads are almost solely borne by the piles. Even so, based on the rules the piles are required to be able to bear all the compression loads from the structure.

On the other hand, the tension loads are almost only balanced by the piles without extra support from other structural members. For the design of traditional offshore oil and gas platforms, tension loads may not occur on the foundation because of the compression provoked by the heavy self-weight of the platform and equipment on top of it. But for an OWT platform, the tension loads are easy to occur because of its relatively light weight and also because the load has a large horizontal component, which makes the tensile load crucial for the axial loads check in the pile design.

3.2. Axial pile performance

When the pile capacity is evaluated, the preliminary dimensions of the pile can be determined. In addition, the obtained pile capacity data is also taken as a benchmark for the further evaluation of the dynamic axial pile performance. To better meet the pile service requirements, axial pile performance is further discussed. This is concerned with the cyclic axial behavior of piles due to operating, structural, and environmental effects. A T-z curve is introduced to evaluate the relative deformations between the soil and the pile in axial direction as shown in Figure 2. A Q–z curve is introduced to evaluate the relatively large pile tip movements (the movements $\geq$ 10% of the pile diameter), as shown in Figure 3. Both the T-z and Q–z curves are obtained from the tabulated data from API rule [10].

3.3. Reaction of soil piles under lateral loads

The lateral loads are resisted by bending moments of the piles as well as passive supports from the surrounding soil, which presents a soil-structure interaction problem. The soil resistance and the pile displacement depend on each other. P-y curves describe the relationship between lateral soil resistance and lateral displacement, which can be calculated from:

$$p = A \times p_u \tanh\left[\frac{k \times z}{A \times p_u}\right] \tag{2}$$

where $A = 0.9$ for cyclic loading; p_u is the ultimate lateral resistance at depth z; k is the rate of increase with depth of initial modulus of subgrade reaction; y is the lateral deflection at depth z; z is the depth below the original seafloor.

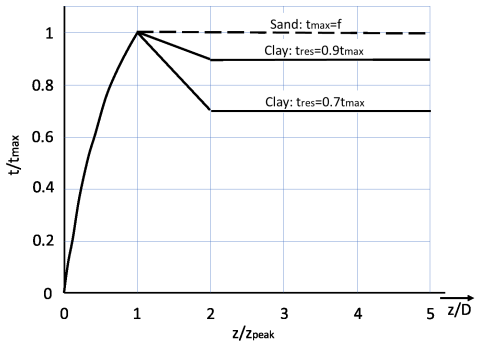

Figure 2: Typical axial pile load—displacement (t-z) curves, where z is the local pile axial deflection; D is the pile outside diameter; t is the mobilized soil-pile adhesion; $t_{\max}$ is the maximum soil pile adhesion or unit shaft friction that equals $f(z)$; t_{res} is the residual soil-pile adhesion or unit shaft friction; z_{peak} is the displacement to maximum soil pile adhesion or unit skin friction; z_{res} is the axial pile displacement at which the residual soil-pile adhesion t_{res} is reached. (adapted from [10])

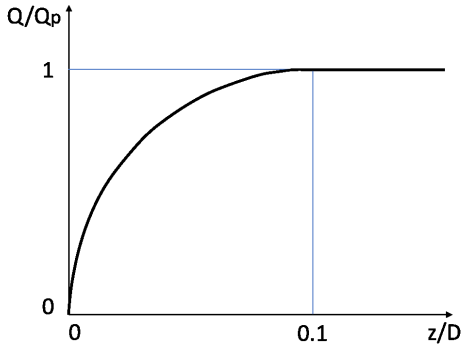

Figure 3: Pile end bearing capacity-displacement curve, where z is the axial pile tip displacement; Q is the mobilized end bearing capacity, in force units; Q_{p} is the the end bearing capacity, in force units. (adapted from [10])

4. A brief introduction of the X-rotor model

The model of the whole wind turbine system is implemented in the multi-body simulation tool Fedem Windpower (Version R7.2.2, Fedem Technology AS) as shown in Figure 4. The primary rotor is modeled as a rigid body, which is driven by the aerodynamic loads on the blades. The rotational speeds of the primary rotor are regulated to the designed rotational speeds at the corresponding wind speeds (8 rpm for rated and above-rated wind speeds) with a controller. The controller is able to regulate the thrusts of the two secondary rotors until the torque of the primary rotor is balanced at the target rotational speed.

It should be noted that the control model used here is to balance the prescribed aerodynamic loads applied on the primary rotor, and is different from the real control strategy of the X-rotor wind turbine. For the real X-rotor wind turbine, the torque of the primary rotor can be balanced by the thrusts of the two secondary rotors and the turbine can reach stable state of rotation speeds with corresponding wind speeds.

In the FEDEM model, the rotor part is connected to the tower part with a revolutionary joint. The tower part and the jacket part are modeled as rigid steel structures. The piles are modeled as interconnected beam sections, connected by joints with nonlinear spring characteristics to

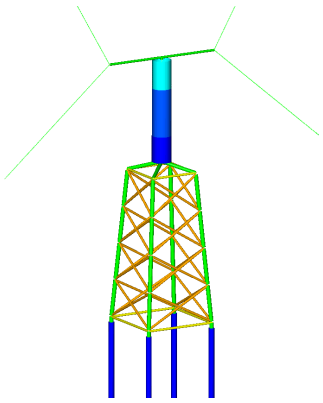

Figure 4: The X-rotor model in FE-DEM, with secondary rotors omitted and a simplified transition piece.

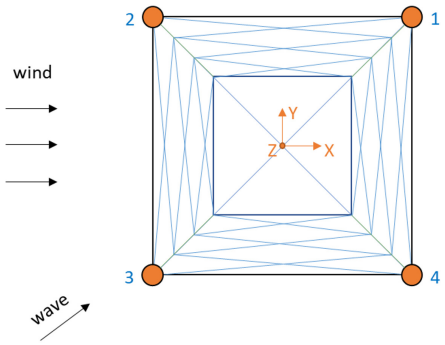

Figure 5: Plan view of the turbine

simulate the soil-pile interaction effects.

5. Results

For the convenience of showing the results, the legs of the jacket and the corresponding piles are numbered as shown in Figure 5, with the global coordinate system satisfying the right-hand rule.

5.1. Pile capacity design

The pile capacity design results are shown in this section. First, the time domain response of the wind turbine without piles is simulated, with the bottom of the legs rigidly clamped to the seafloor. The maximum and minimum loads at the lower end of the jacket legs are summarized in Table 3, with the negative values representing the pullout loads. The most critical loads, shown in bold font, are considered for the pile capacity design, with a ULS safety factor of 1.25 [9].

Table 3: Extreme vertical loads at the lower end of the jacket legs

DLC	MaxF_v(kN)	Leg	MinF_v(kN)	Leg
1	**17420**	2	**-3638**	4
2	17233	2	-3397	4
3	17353	2	-3626	4
4	16993	2	-3210	4
5	**17420**	2	-1759	1
6	12043	3	642	1
7	11957	4	693	2
8	11406	1	715	3
9	13717	2	-745	4
10	11109	2	1768	1

The capacity curves of the pile are shown in Figure 6. It shows that the pile should be designed to withstand both the compression and pullout loads with a combination of the lengths and diameters above the red line.

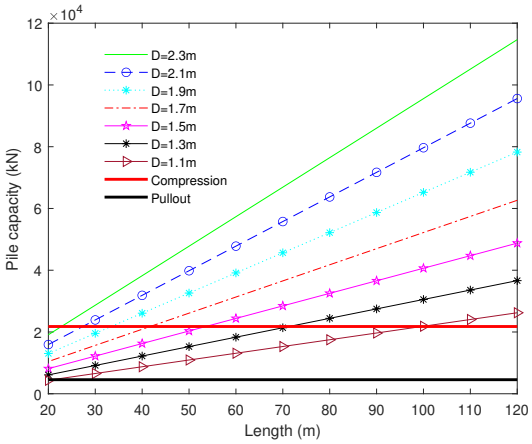

Figure 6: Pile capacity design is executed with different combinations of length and diameter of a series of piles; a ULS safety factor of 1.25 is considered for the compression and pullout loads here

5.2. Pile performance design

The pile performance design results are shown in this section. Taking DLC 1 as an example, Figures 7-9 show the time domain response of the lateral displacements on the top end of the pile. Figures 7 and Figures 8 show piles with different thicknesses, and Figures 7 and Figures 9 show piles with different diameters.

Theoretically, the thickness of the pile has direct influence on the pile tip resistance which reflects on the Q-z curve, as well as the stiffness of the pile itself. Meanwhile, the pile diameter has influence on the pile tip resistance, axial resistance, lateral resistance of the pile-soil system, as well as the stiffness of the pile itself. Thus the value of the pile diameter would have a more significant effect on the pile performance. However, to limit the horizontal displacement at the pile head, either increasing the thickness or the diameter can gain a significant effect. As shown in Figure 7, the maximum amplitude of the pile top displacement is more than 0.1 m. After increasing the thickness of the pile from 2 cm to 4 cm, the maximum amplitude of the pile top displacement becomes 0.02 m, as shown in Figure 8. Or increasing the diameter of the pile from 2.3m to 2.4m, the maximum amplitude of the pile top displacement is reduced to 0.015 m, as shown in Figure 9. These two strategies are both effective.

From these results, we conclude that the pile top displacement largely depends on the pile stiffness itself rather than the lateral support from the soil. The relationship between the mass, stiffness and pile top displacement will be discussed later.

5.3. The influence of the piles on the natural frequencies of the wind turbine

As mentioned before, the pile-soil interaction effect has influence to the natural frequency f_n of the whole wind turbine system. To evaluate this influence, the flexibility coefficient C_J is introduced, which represents the following relationship

$$f_n = f_{fb} C_J \tag{3}$$

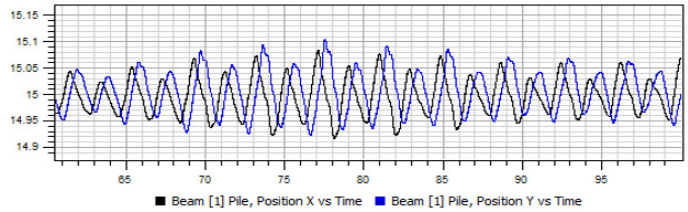

Figure 7: Pile top displacement (m) with pile L100m, D2.3m, t2cm of leg 1 and DLC 1

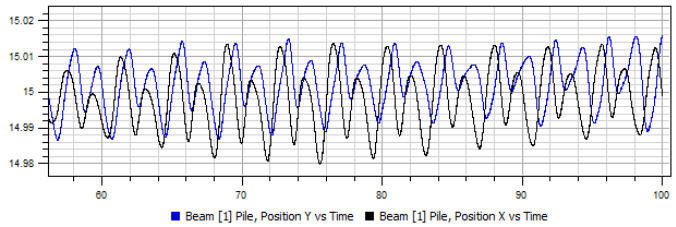

Figure 8: Pile top displacement with pile L100m, D2.3m, t4cm of leg 1 and DLC 1

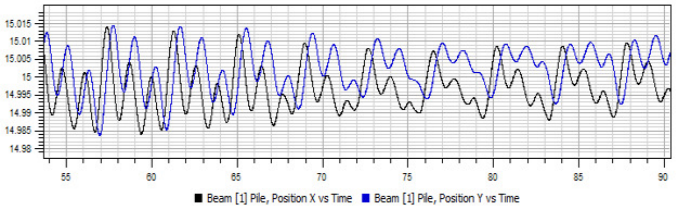

Figure 9: Pile top displacement with pile L100m, D2.4m, t2cm of leg 1 and DLC 1

where f_{fb} is the target design frequency of the fixed based tower-jacket system without piles. C_J is calculated with a series of empirical formulas as introduce in [15].

$$C_J = \sqrt{\frac{\tau}{\tau + 3}} \tag{4}$$

$$\tau = \frac{k_R h_{total}}{EI_{T-J}} \tag{5}$$

$$k_R = k_v L_{bottom}^2 \left[\frac{\alpha}{1+\alpha}\right] \tag{6}$$

$$k_v = \frac{2\pi L_p G_s}{\zeta} \tag{7}$$

where EI_{T-J} is the bending stiffness of the tower-jacket system, h_{total} is the total height of the tower-jacket system, L_{bottom} is the jacket leg bottom spacing, α is the foundation stiffness variability factor taken as 1, k_v is the vertical stiffness of the foundation, G_s is the average of the sandy soil shear modulus between the top and bottom of the pile, which is taken as 30 MPa according to Fig.17 in [15] corresponding to a soil depth of 30m, L_p is the length of the pile taken as 60 m, ζ is the damping ratio relative to critical damping taken as 4. Based on the current design, EI_{T-J} can be estimated according to the main dimensions and target frequency of the jacket-tower system as:

$$EI_{T-J} = \frac{1}{3}(2\pi f_{fb})^2(0.243 m_{eq} h_{total} + M_{RNA})(h_{total})^3$$
$$= \frac{1}{3}(2\pi \times 0.3)^2(0.243 \times 27155 \times 113 + 128166)113^3 = 1.5 \times 10^{12}(\mathrm{Nm}^2)$$

where m_{eq} is the equivalent distributed mass of the tower-jacket system and M_{RNA} is the lumped mass of the rotors. Based on these conditions C_J is calculated with a given range of EI_{T-J} as shown in Figure 10.

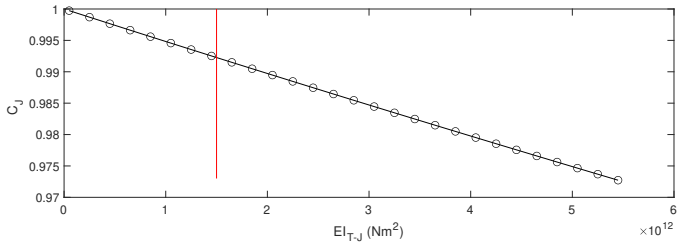

Figure 10: Variation of flexibility coefficient C_J with bending stiffness EI_{T-J} of the tower-jacket system; the red line marks the estimated EI_{T-J} so far.

With the combination of the chosen values of all these parameters, C_J and EI_{T-J} have an almost linear relationship at this stage. But it should be noted that the change of any parameters above would change the shape of the curve in Figure 10. With the estimated value of EI_{T-J} as $1.5 \times 10^{12}\mathrm{Nm}^2$ for the current design, C_J equals to 0.992, which means that f_{fb} is reduced to $0.992 f_{fb}$ with the effect of the pile foundation. If the stiffness of the jacket-tower system further increases, the natural frequency will be reduced more significantly by the pile foundation, vice versa.

6. Conclusion

The ULS design process of the pile foundation of the X-rotor wind turbine is described. Firstly, the pile capacity design is executed, which considered the axial static load and the pile tip resistance. Particularly, the pullout load is seen in the simulation as expected. Secondly, the pile performance analysis is executed, which considered the cyclic loads from both the axial direction and the lateral directions. The way to limit the amplitudes of the lateral displacement is discussed. The influence of the piles to natural frequencies of the wind turbine is also evaluated. With these evaluations it is possible to find a suitable pile design even for these larger loads.

However, in order to be able to more accurately define the pile design from the cost reduction point of view, the fatigue life and a mass sensitivity analysis will need to be performed, where the soil state changes due to cyclic loads will be payed particular attention to.

7. Acknowledgement

We acknowledge the funding of the X-ROTOR project from the European Union's Horizon 2020 Programme for Research and Innovation under Grant Agreement No. 101007135.

We acknowledge the aerodynamic group of the X-rotor project in TU Delft for their diligent support by providing aerodynamic data for the wind turbine dynamic response simulation.

8. Authors' Contributions

JD wrote the manuscript of the paper, composed the model, developed the methodology for the design, conducted analyses, postprocessing, and executed the pile design; ACDS prepared the aerodynamic loads for the analysis, provided the FEDEM models of the rotor, tower, and jacket; and MM formulated the goals, managed the X-rotor project, modified the draft paper, and approved the version for publication. All authors reviewed the final manuscript.

References

[1] William Leithead et al. "The X-Rotor Offshore Wind Turbine Concept". In: *Journal of Physics: Conference Series* 1356.1 (Oct. 2019), p. 012031. DOI: 10.1088/1742-6596/1356/1/012031.

[2] Gerwick Jr., B.C. "Construction of Marine and Offshore Structures (3rd ed.)" In: 2007, pp. 433–478. DOI: 10.1016/B978-0-08-100779-2.00020-9.

[3] HSE. "A study of pile fatigue during driving and in-service and of pile tip integrity". In: Prepared by MSL Engineering Limited for the Health and Safety Executive. 2001.

[4] Mohamed A. El-Reedy. "3 - Offshore Structures' Loads and Strength". In: *Marine Structural Design Calculations*. Ed. by Mohamed A. El-Reedy. Oxford: Butterworth-Heinemann, 2015, pp. 33–84. ISBN: 978-0-08-099987-6. DOI: https://doi.org/10.1016/B978-0-08-099987-6.00003-9.

[5] Martin Achmus. "Design of Axially and Laterally Loaded Piles for the Support of Offshore Wind Energy Converters". In: 2010.

[6] Lin Li, Zhen Gao, and Torgeir Moan. "Joint Distribution of Environmental Condition at Five European Offshore Sites for Design of Combined Wind and Wave Energy Devices". In: *Journal of Offshore Mechanics and Arctic Engineering* 137.3 (June 2015). ISSN: 0892-7219. DOI: 10.1115/1.4029842.

[7] DNV GL. *Loads and site conditions for wind turbines*. DNVGL-ST-0437. 2016.

[8] A. Correia da Silva and M. Muskulus. "X-Shape Radical Offshore Wind Turbine for Overall Cost of Energy Reduction," in: (9. 2021). WP4 Design of Mechanical Structure and Analysis, T4.2 Establishment of a design basis, D4.1 Design basis.

[9] DNV GL. *Support structures for wind turbines*. DNVGL-ST-0126. 2016.

[10] API. *Geotechnical and Foundation Design Considerations*. ISO 19901-4:2003. 2014.

[11] API. *Planning, Designing, and Constructing Fixed Offshore Platforms—Load and Resistance Factor Design*. API Recommended Practice 2A-LRFD Second Edition, 08 2019.

[12] API. *Planning, Designing, and Constructing Fixed Offshore Platforms—Working Stress Design*. API Recommended Practice 2A-WSD Twenty-second Edition, 11 2014.

[13] Kenneth Gavin, David Igoe, and Paul Doherty. "Piles for offshore wind turbines: a state-of-the-art review". In: *Proceedings of the Institution of Civil Engineers - Geotechnical Engineering* 164.4 (2011), pp. 245–256. DOI: 10.1680/geng.2011.164.4.245.

[14] *An Efficient Solution to Mudmat Design for Jacket Structures in Soft Seabed Soil*. Vol. Day 1 Tue, October 12, 2021. SPE Asia Pacific Oil and Gas Conference and Exhibition. Oct. 2021. DOI: 10.2118/205529-MS.

[15] Saleh Jalbi and Subhamoy Bhattacharya. "Concept design of jacket foundations for offshore wind turbines in 10 steps". In: *Soil Dynamics and Earthquake Engineering* 139 (2020), p. 106357. ISSN: 0267-7261. DOI: https://doi.org/10.1016/j.soildyn.2020.106357.